

AD-A121 446

SINGLE PARTICLE IMPACT TESTING ALTERNATE MATERIALS
STUDY(U) AEROJET LIQUID ROCKET CO SACRAMENTO CA
W B ARNOLD APR 82 ALRC-3215-30 BMO-TR-82-36

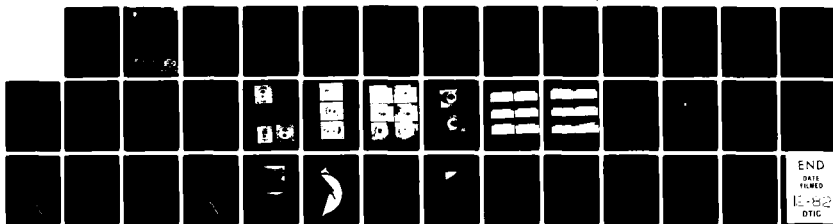
11

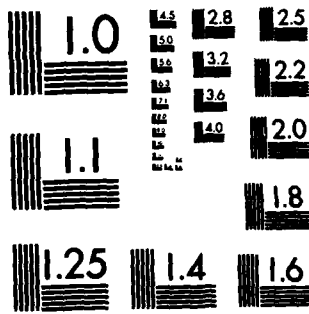
UNCLASSIFIED

F04704-80-C-0022

F/G 11/6

NL





MICROCOPY RESOLUTION TEST CHART
NATIONAL BUREAU OF STANDARDS-1963-A

AD A 121 446

NOT FULL COPY

FOREWORD

This final report was submitted by Aerojet Liquid Rocket Company, Sacramento, CA, under contract F04704-80-0022 with the Ballistic Missile Office, AFSC, Norton AFB, CA. Major Kevin E. Yelmgren, BMO/SYMS was the project officer in charge. This technical report has been reviewed and is approved for publication.

Kevin E. Yelmgren
KEVIN E. YELMGREN, Major, USAF
Chief, Advanced Systems Division
Advanced Strategic Missile Systems

FOR THE COMMANDER

Richard T. Williams
RICHARD T. WILLIAMS, Lt Col, USAF
Director, Missile Systems
Advanced Strategic Missile Systems

| | |
|--------------------|-------------------------------------|
| Accession For | |
| NTIS GRA&I | <input checked="" type="checkbox"/> |
| DTIC TAB | <input type="checkbox"/> |
| Unannounced | <input type="checkbox"/> |
| Justification | |
| By _____ | |
| Distribution/ | |
| Availability Codes | |
| Dist | Avail and/or Special |
| A | |



TABLE OF CONTENTS

| | <u>Page</u> |
|--------------------------------------|-------------|
| I. Introduction | 1 |
| II. Discussion | 1 |
| III. Conclusions and Recommendations | 31 |
| Distribution List | 33 |

LIST OF FIGURES

| <u>Figure No.</u> | <u>Title</u> | <u>Page</u> |
|-------------------|---|-------------|
| 1 | Crater Symmetry for TZM | 8 |
| 2 | Crater Volume Vs. Temperature for TZM and Moly | 10 |
| 3 | Craters in TZM from Impact | 11 |
| 4 | Crater Photomicrograph in TZM | 12 |
| 5 | Crater Photomicrograph in Molybdenum | 13 |
| 6 | Crater Photomicrograph in TZM | 14 |
| 7 | Shadowgraphs of Crater Rims | 15 |
| 8 | Shadowgraphs of Crater Rims | 16 |
| 9 | Crater Mapping Technique | 18 |
| 10 | TZM Crater Contour Plot | 19 |
| 11 | TZM Crater Cross-Section Plot | 20 |
| 12 | Depth Vs. Radius Plot of Crater in TZM | 21 |
| 13 | Molybdenum Crater Contour Plot | 22 |
| 14 | Molybdenum Crater Cross-Section Plot | 23 |
| 15 | Depth Vs. Radius Plot of Crater in Molybdenum | 24 |
| 16 | Photomicrograph Bottom of Crater in TZM | 25 |
| 17 | Photomicrograph Bottom of Crater in Molybdenum | 25 |
| 18 | Photomicrograph Composite of Crater in Molybdenum | 26 |
| 19 | Photomicrograph TZM Specimen from Test E4422 | 27 |
| 20 | Photomicrograph Molybdenum Specimen from Test E4420 | 28 |
| 21 | Relative Erosion Coefficients for Molybdenum, TZM, Tungsten and 347 Stainless Steel | 30 |

LIST OF TABLES

| <u>Table No.</u> | | <u>Page</u> |
|------------------|--|-------------|
| I | ETI Exploding Wire Test Facility Diagnostic Capabilities | 2 |
| II | Measured Crater Dimensions for TZM | 4 |
| III | Measured Crater Dimensions for Molybdenum | 5 |
| IV | Data Summary TZM Impact Tests | 6 |
| V | Data Summary Molybdenum Impact Tests | 7 |
| VI | Microhardness of TZM and Molybdenum | 29 |

I. INTRODUCTION

The purpose of the single particle impact testing was to obtain erosion data on two potential advanced nosetip materials, pure Molybdenum (ABL-2) and Molybdenum TZM (ABT-3). The data obtained were reduced to an erosion coefficient/temperature relationship $C_n(T)$, and compared to existing data for stainless steel.

The testing was accomplished at the Effects Technology Inc., Hypervelocity Test Facility under Contract F04701-77-C-0130.

II. DISCUSSION

Hypervelocity impact testing has been completed on two candidate TCNT materials: TZM and Molybdenum. Twelve planned tests were conducted with a nominal glass particle diameter of 1mm at 12 kft/sec. Duplicate tests were conducted at 70, 1800 and 3000 degrees Fahrenheit for a total of six tests per material. The TZM test series preceded the Molybdenum test series because of the sequence in which the materials for the test specimens were received. Gravimetric mass loss measurements were not made for this first series of TZM tests. Following review and analysis of this first TZM data set, the necessity of measuring gravimetric mass loss in addition to volumetric mass loss became apparent. A relatively large amount of material had displaced from the crater region to form a raised lip surrounding the crater. Therefore, two additional TZM tests, one at 70°F, and one at 3000°F were conducted to obtain the needed gravimetric mass loss measurement for comparison to the Molybdenum data. Fourteen tests in all were conducted for this effort.

The data obtained during these tests consisted of measurements of particle mass, impact velocity, specimen temperature, volume loss, and mass loss. The accuracy of these measurements is summarized in Table 1.

TABLE 1

ETI EXPLODING-WIRE EROSION TEST FACILITY
DIAGNOSTIC CAPABILITIES

| Measured Quantity | Method | Accuracy |
|-----------------------|-------------------|----------|
| Particle diameter | Microscope | ± 2% |
| Particle mass | Microbalance | ± 1 µg |
| Particle mass | Microscope | ± 6% |
| Mass loss | Microbalance | ± 1 µg |
| Impact velocity | Framing camera | ± 5% |
| Impact location (aim) | Laser alignment | ± 500 µ |
| Specimen temperature | Optical pyrometer | ± 14°C |
| Crater volume | Mercury Fill | ± 2% |
| Crater volume | Microscope | ± 5% |

Crater depth, diameter, and rim height measurements were also made on each test. A summary of this data is presented in Tables II and III for the TZM and Molybdenum materials, respectively. These data represent maximum measured values.

A summary of the impact test results for both the TZM and Molybdenum material is presented in Tables IV and V, respectively. Table IV contains the data obtained from the first series of TZM tests which did not include gravimetric mass loss measurements. Table V contains the Molybdenum data and the two additional TZM data points. These tables include the test conditions for each test as well as the calculated mass loss ratios and the corresponding erosion coefficients. The formulas used to make these calculations are listed at the bottom of Table IV. The data are normalized to a reference condition of 12kft/sec using the common V-squared relationship, thereby correcting the mass loss data for experimental variations in the impact velocity and particle mass.

The mass lost was determined by 1) weighing the specimen before and after testing, 2) determining a total crater volume using a mercury fill technique and then calculating the mass lost, and 3) mapping the crater profile with a microscope (depth versus radius) and calculating the subsurface crater volume by adding the calculated volumes of concentric cylinders. The volume calculation from this measurement technique was possible due to the crater symmetry shown in Figure 1. This figure presents an overlay of two crater depth profiles obtained from the same crater but in orthogonal directions.

Actual gravimetric mass loss measurements were made on only eight tests, while volume measurements were made for all fourteen tests. It was anticipated that the gravimetric measurements for tests conducted at elevated temperatures would result in higher mass loss values due to heating. A 3000 degree tare test was conducted on a Molybdenum sample to measure this mass loss contribution due to heating. The results of this test showed a 3.2 milligram mass loss. As indicated in Table V, the actual measured mass loss for two of the three

TABLE II

MAXIMUM MEASURED CRATER DIMENSIONS FOR T2M (ABT-3)
 MATERIALS IMPACTED AT 12 kft/sec WITH A 1 mm GLASS SPHERE

| Test No. | Crater Dimensions | | | Temp. |
|----------|--|---|--|-----------------------------|
| | Depth $P \pm 10$ (μm) | Diameter $D \pm 50$ (μm) | Rim $L \pm 10$ (μm) | T ($^{\circ}\text{F}$) |
| E4409 | 790 | 2190 | 290 | 1800 |
| E4413 | 760 | 2110 | 300 | 1800 |
| E4414 | 540 | 1960 | 260 | 70 |
| E4415 | 550 | 1910 | 260 | 70 |
| E4416 | 870 | 2260 | 370 | 3000 |
| E4417 | 900 | 2320 | 370 | 3000 |
| E4422 | 550 | 1710 | 230 | 70 |
| E4430 | 800 | 2100 | 320 | 3000 |

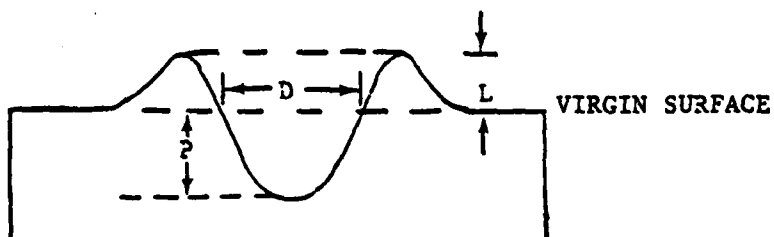


TABLE III

MAXIMUM MEASURED CRATER DIMENSIONS FOR MOLYBDENUM (ABL-2)
MATERIALS IMPACTED AT 12 kft/sec WITH A 1 mm GLASS SPHERE

| Test No. | Crater Dimensions | | | Temp. |
|----------|--|---|--|-----------------------------|
| | Depth $P \pm 10$ (μm) | Diameter $D \pm 50$ (μm) | Rim $L \pm 10$ (μm) | T ($^{\circ}\text{F}$) |
| E4419 | 580 | 2060 | 260 | 70 |
| E4420 | 600 | 1940 | 250 | 70 |
| E4426 | 850 | 2060 | 300 | 1800 |
| E4427 | 800 | 2160 | 280 | 1800 |
| E4428 | 920 | 2450 | 320 | 3000 |
| E4429 | 920 | 2310 | 360 | 3000 |

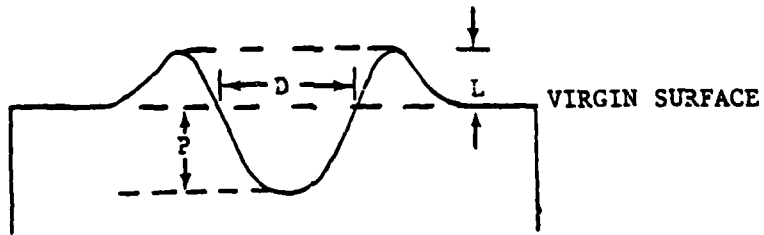


TABLE IV.

DATA SUMMARY OF 1.0 mm GLASS SPHERE IMPACT TESTS
 CONDUCTED ON TZM (ABT-3) MATERIAL ($\rho_0 = 10.15 \text{ gm/cm}^3$)

| Test No. | Impact Velocity | | Particle Mass M_p (mg) | Specimen Temp T ($^{\circ}\text{F}$) | Volume Loss V_c (mm^3) | Volumetric ^a Mass Loss | | Normalized ^{**} | | | Erosion Coefficient C_N^+ (Joules/gm) | | |
|----------|-----------------|----------|--------------------------|--|-------------------------------------|-----------------------------------|----------------|-----------------------------|--|-----------------------------|---|--|------|
| | V_p (kft/sec) | (km/sec) | | | | M_{Vc} (mg) | M_{Vcs} (mg) | Volume Loss Ratio V_c/V_p | Mass Loss Ratio G_V^{12}/G_{CS}^{12} | Volume Loss Ratio V_c/V_p | | Mass Loss Ratio G_V^{12}/G_{CS}^{12} | |
| E4409 | 13.5 | 4.11 | 1.367 | 1800 | 2.9 | 1.6 | 29.4 | 16.2 | 4.2 | 2.3 | 16.9 | 9.3 | 710 |
| E4413 | 12.7 | 3.87 | 1.453 | 1800 | 2.7 | 1.5 | 27.4 | 15.2 | 4.2 | 2.3 | 16.7 | 9.1 | 720 |
| E4414 | 12.8 | 3.90 | 1.498 | 70 | 1.6 | 0.8 | 16.2 | 8.1 | 2.4 | 1.2 | 9.8 | 4.8 | 1410 |
| E4415 | 12.9 | 3.93 | 1.473 | 70 | 1.7 | 0.8 | 17.2 | 8.1 | 2.5 | 1.2 | 10.0 | 4.6 | 1400 |
| E4416 | 12.5 | 3.81 | 1.473 | 3000 | 3.7 | 1.6 | 37.6 | 16.2 | 5.8 | 2.5 | 23.3 | 10.1 | 660 |
| E4417 | 12.9 | 3.93 | 1.458 | 3000 | 4.0 | 1.8 | 40.6 | 18.3 | 6.0 | 2.7 | 42.0 | 10.7 | 615 |

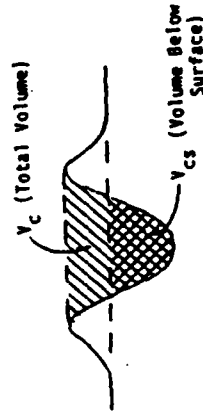
^a Volumetric Mass Loss, (M) = Volume Loss (V) x Material Density (ρ_0)

^{**} Data Normalized to 12 kft/sec as follows: $G^{12} = \frac{M^{12}}{M_p} = \frac{M}{M_p} \left(\frac{12}{V}\right)^2 \cdot \frac{V^{12}}{V_g} = \frac{V}{V_g} \left(\frac{12}{V}\right)^2$

⁺ Erosion coefficient calculated as follows: $C_N^+ = \frac{(V_p)^2}{2 \frac{M_{Vcs}}{M_p} \times 1000} \text{ Joules/Gm}$

Legend

- V_c = Total crater volume
- V_{cs} = Subsurface crater volume
- V_g = Volume of glass sphere
- where V_p = M/sec
- M_{Vcs} = Milligrams
- M_p = Milligrams



$V = 12 \text{ kfps}$
 $\theta = 90^{\circ}$
 1.0 mm diameter glass particle

TABLE V

DATA SUMMARY OF 1.0 mm GLASS SPHERE IMPACT TESTS
 CONDUCTED ON POLYBUTEN (ABL-2) MATERIAL ($\rho_0 = 10.20 \text{ gm/cm}^3$)
 AND TZH (ABT-3) MATERIAL

| Test No. | Impact Velocity | | Particle Mass M_p (mg) | Specimen Temp T ($^{\circ}\text{F}$) | Volume Loss | | Volumetric ^a Mass Loss | | Gravimetric Mass Loss G_{CS} (mg) | Normalized ^{**} | | | Erosion Coefficient C_{Rv} C_{Cs} | | | |
|-------------------|------------------------|----------------------|--------------------------|--|-------------------------|----------------------------|-----------------------------------|----------------|-------------------------------------|---|--|---|---------------------------------------|-------------------|------|--------|
| | (kft/sec) ^b | (M/sec) ^b | | | V_c (mm^3) | V_{cs} (mm^3) | M_{vc} (mg) | M_{vcs} (mg) | | Volume Loss Ratio $\left[\frac{V_c^{12}/V_{cs}}{C_{Rv}}\right]$ | Volumetric Mass Loss Ratio $\left[\frac{M_{vc}^{12}}{C_{Cs}}\right]$ | Gravimetric Mass Loss Ratio $\left[\frac{G_{cs}^{12}}{C_{Cs}}\right]$ | | | | |
| M O L Y B D E U M | 12.7 | 3.87 | 1.482 | 70 | 1.8 | 0.87 | 18.4 | 8.9 | 0.7 | 2.8 | 1.3 | 11.1 | 5.4 | 0.47 | 1250 | 15,930 |
| | 12.8 | 3.90 | 1.476 | 70 | 2.0 | 0.85 | 20.4 | 8.7 | 0.7 | 3.0 | 1.3 | 12.1 | 5.2 | 0.47 | 1290 | 16,180 |
| | 12.7 | 3.87 | 1.318 | 1800 | 3.2 | 1.2 | 32.6 | 12.1 | 0 | 5.5 | 2.0 | 22.1 | 8.2 | 0 | 820 | -- |
| | 12.4 | 3.78 | 1.315 | 1800 | 2.8 | 1.20 | 28.6 | 12.3 | 0.1 | 5.1 | 2.2 | 20.4 | 8.1 | 0.08 | 740 | -- |
| | 13.0 | 3.96 | 1.315 | 3000 | 3.9 | 1.51 | 39.8 | 15.7 | 26.0 [†] | 6.4 | 2.5 | 25.8 | 10.2 | 19.8 [†] | 660 | -- |
| | 12.7 | 3.87 | 1.315 | 3000 | 3.8 | 1.60 | 38.8 | 16.3 | 3.0 [†] | 6.6 | 2.8 | 26.3 | 11.1 | 2.30 [†] | 600 | -- |
| T Z H | 12.7 ^a | 3.87 | 1.498 | 70 | 1.6 | 0.48 | 16.2 | 4.9 | 1.1 | 2.4 | 0.73 | 9.6 | 3.3 | 0.73 | 2270 | 10,260 |
| M | 12.7 ^a | 3.87 | 1.318 | 3000 | 3.0 | 1.30 | 30.4 | 13.2 | 3.0 | 5.2 | 2.24 | 20.6 | 10.0 | 2.30 | 750 | -- |

^{**} Data normalized to 12 kft/sec (see Table 4).

^a Calibrated velocity--cameras misfired--no high speed photography.

[†] A heat only test conducted at 3000 $^{\circ}\text{F}$ resulted in 3.2 milligrams of mass loss; consequently 3.2 milligrams must be subtracted from these values.

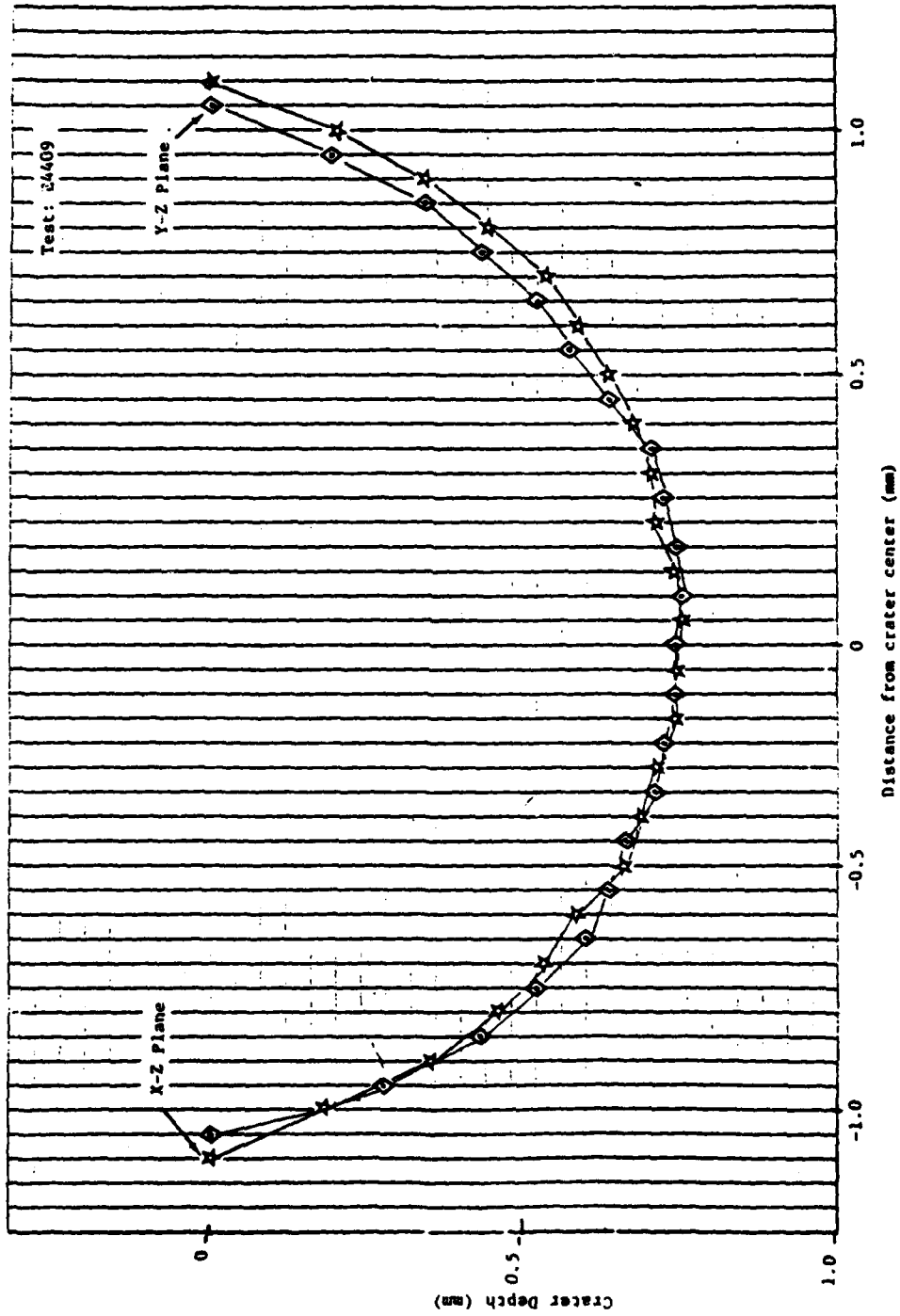


Figure 1. Plot showing crater symmetry as crater depth versus distance from the crater center for measurements made on T2H material in the X-Z and Y-Z orthogonal planes.

2

impact tests conducted at 3000 degrees, one being TZM and the other Molybdenum material, was 3 milligrams. This indicates that the effective mass loss resulting solely from the impact is probably very small, much less than that using the measured volume displaced below the cratered surface. The other high temperature Molybdenum impact test (E4428) produced anomalous results.

The mass loss due to heating probably is not the same on each high temperature test due to differences in the gas environment that the specimen was exposed to during heating. An attempt was made to reduce the oxidation by providing an inert atmosphere using Argon gas during the test. However, the dewpoint of the argon gas used is unknown and the method of introducing the Argon into the test chamber does not preclude the presence of air/oxygen in the chamber during the test. The presence of oxygen or moisture will greatly affect the material oxidation and as a result the mass loss will vary from test to test.

The apparent differences between the measured gravimetric mass loss and the mass loss calculated from the subsurface crater volume measurement are probably due to the transfer of mass to the crater rim. Consequently, the erosion coefficient calculated from the volume measurement does not reflect the mass lost but the mass displaced from the crater. The relationship between total crater volume and subsurface crater volume for both the TZM and Molybdenum materials is plotted versus temperature in Figure 2.

Photomicrographs of the craters resulting from all fourteen 1mm glass particle impact tests at 12kft/sec are presented in Figures 3, 4, 5 and 6 for both materials. Shadowgrams of the crater rims (sideview) for each test are included in Figures 7 and 8.

Additional crater mapping was accomplished on TZM and Molybdenum specimens from test numbers E4417 and E4429. These specimens were selected because they were subjected to testing at 3000°F and the test conditions are

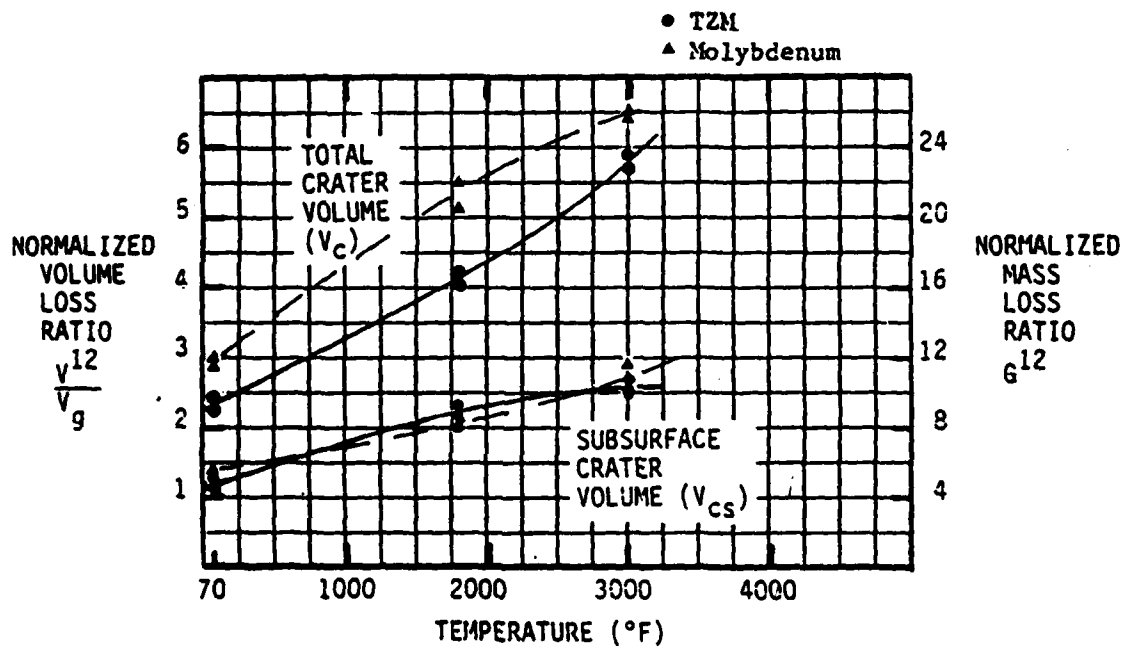
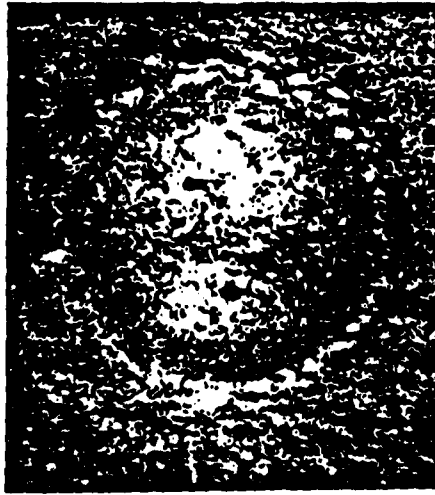
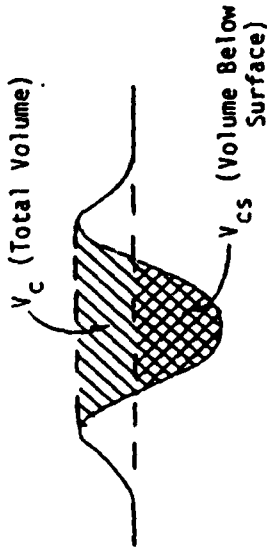


Figure 2. Plot of total (V_c) and subsurface (V_{cs}) crater volumes versus temperature for TZM and Molybdenum resulting from a 1mm glass sphere impact at 12 kft/sec.

CRATERS IN TZM FROM HYPERVELOCITY IMPACT



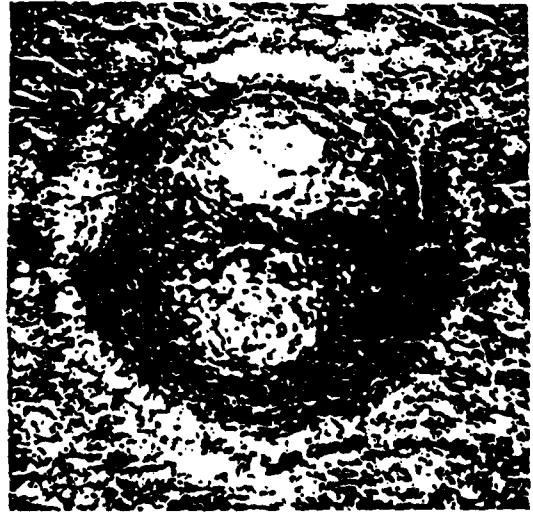
70°F $V_c = 1.66 \text{ mm}^3$ $V_{cs} = 0.79 \text{ mm}^3$



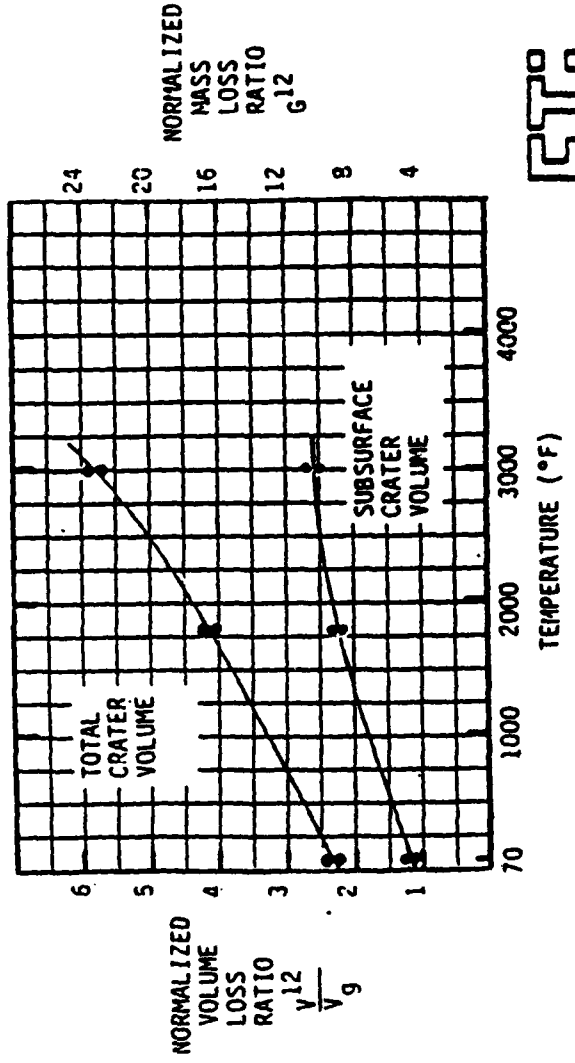
$V = 12 \text{ kfps}$
 $\theta = 90^\circ$
 1.0 mm diameter glass particle



1800°F $V_c = 2.78 \text{ mm}^3$ $V_{cs} = 1.52 \text{ mm}^3$

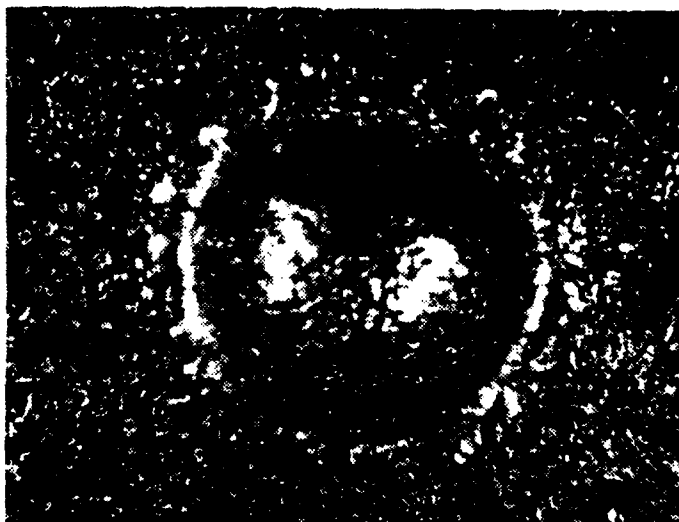


3000°F $V_c = 3.84 \text{ mm}^3$ $V_{cs} = 1.68 \text{ mm}^3$

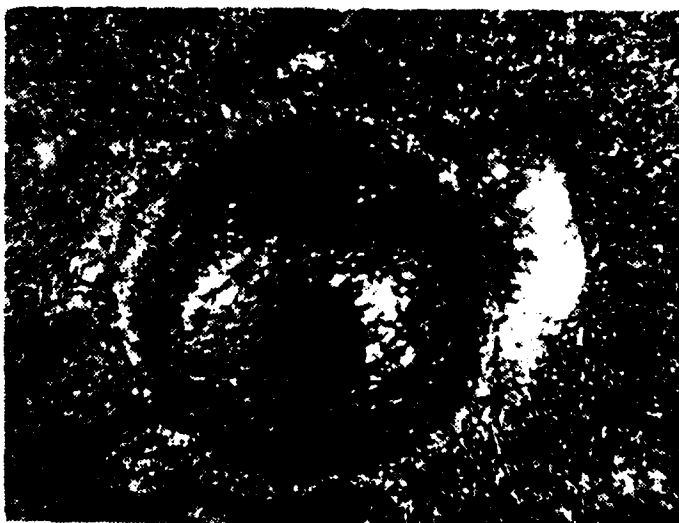




E4414
70°F
19.5 x Magn.



E4413
1800°F
19.5 x Magn.



E4416
3000°F
19.5 x Magn.

Figure 4. Photomicrographs of Craters Resulting from 1.0 mm Glass Sphere (90°) Impact Tests on TZM (ABT) Material Conducted at 12 kft/sec.

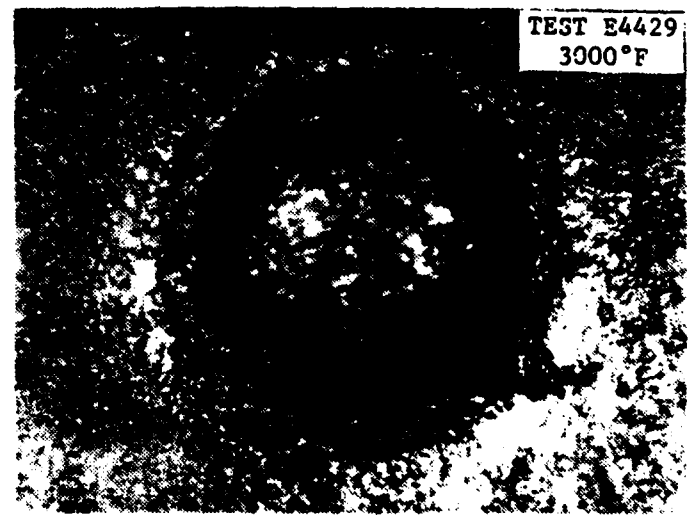
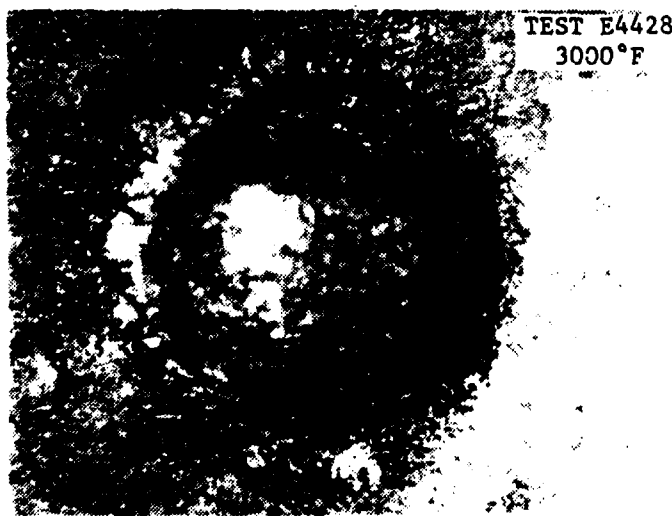
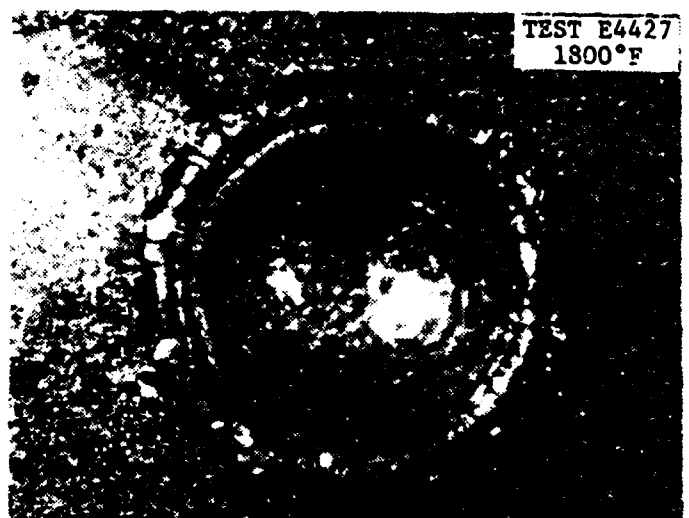
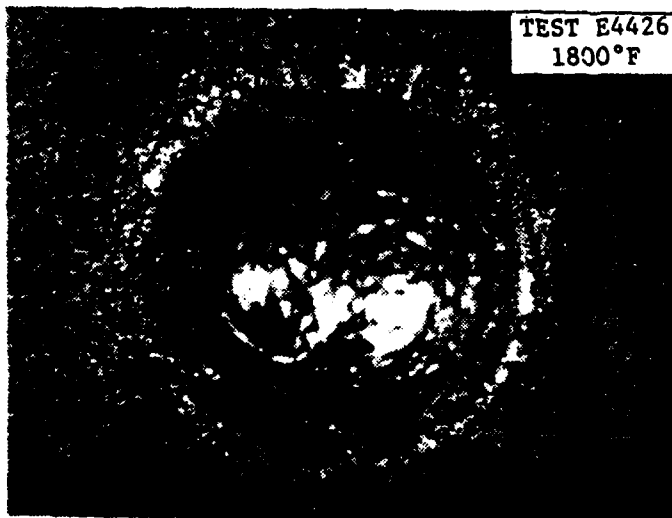
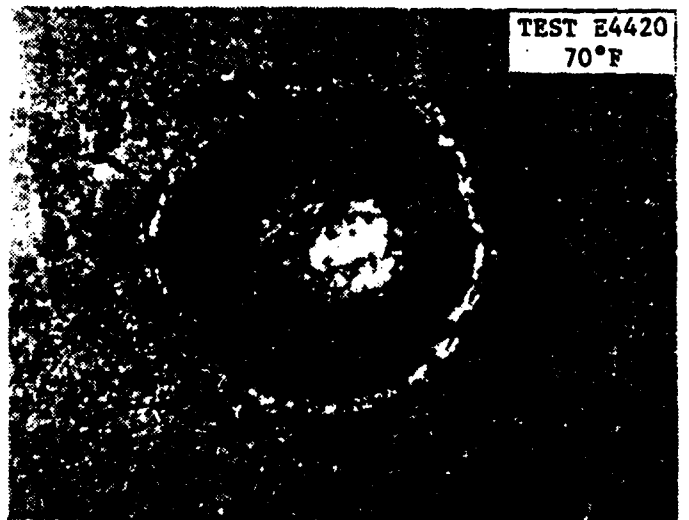
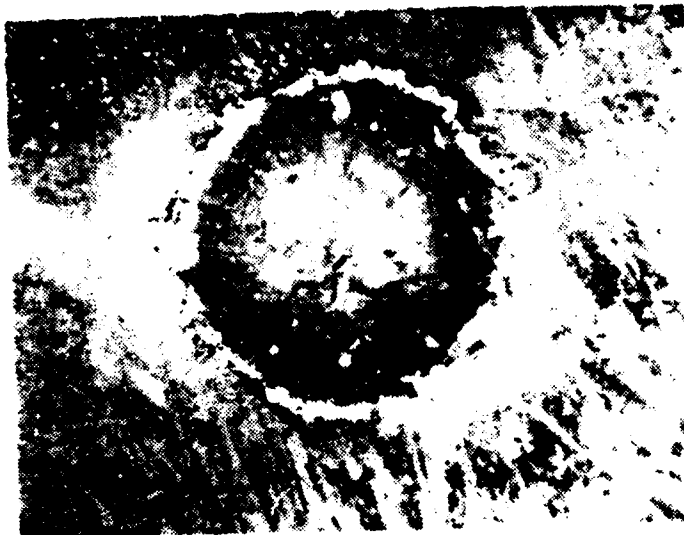


Figure 5. Photomicrographs of Craters in Molybdenum Resulting from 1 mm Glass Sphere Impacts at 12 kft/sec (19.5 x Magn.)

TEST E4422
70°F



TEST E4430
3000°F

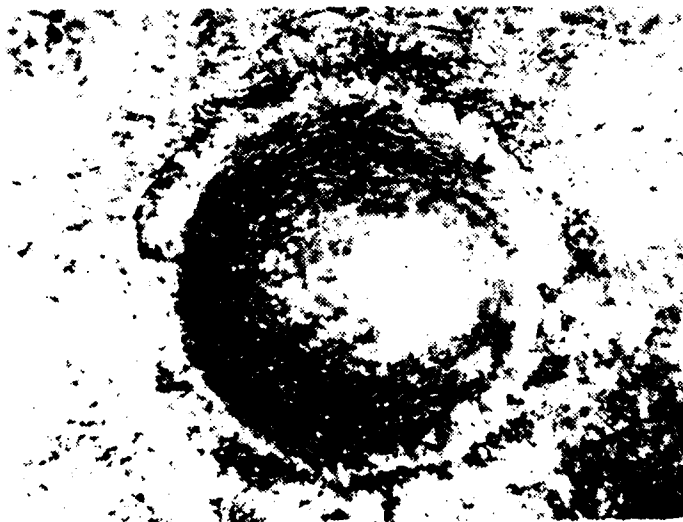


Figure 6. Photomicrographs of Craters in TZM Resulting from a 1 mm Glass Sphere Impact at 12 kft/sec.

TEST E4417
3000°F



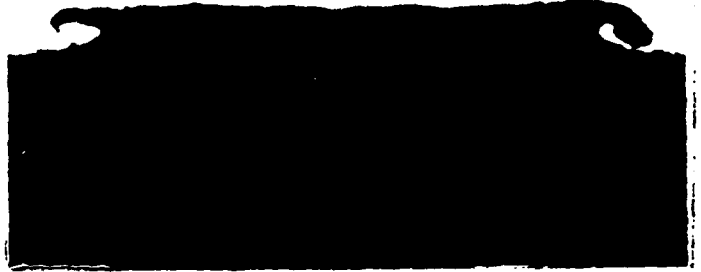
TEST E4416
3000°F



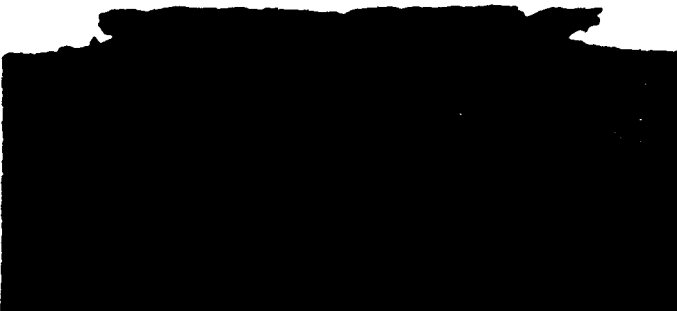
TEST E4409
1800°F



TEST E4413
1800°F



TEST E4414
70°F

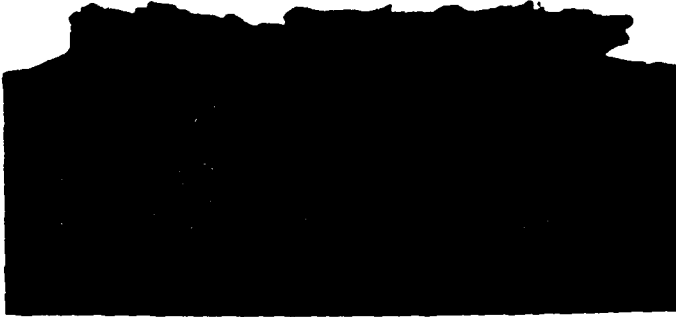


TEST E4415
70°F



Figure 7. Shadowgrams of Crater Rim (Sideview) Protruding Above the Virgin Surface (26 x Magn.)

TEST E4428, 3000°F



TEST E4429, 3000°F



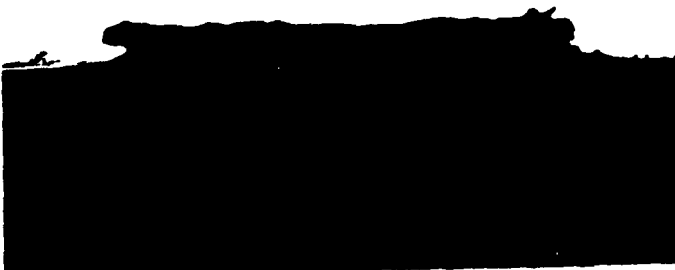
TEST E4426, 1800°F



TEST E4427, 1800°F



TEST E4419, 70°F



TEST E4420, 70°F

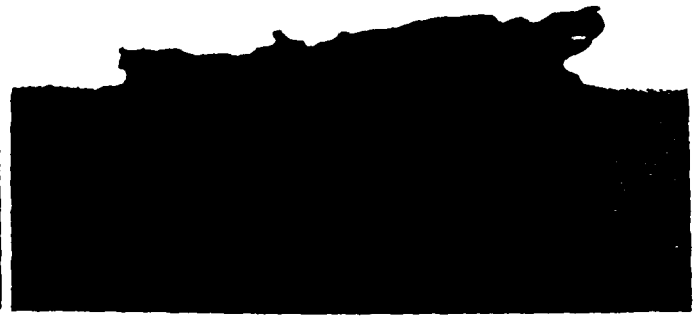


Figure 2. Shadowgrams of Crater Rim (Side View) Protruding Above the Virgin Surface (26 x Magn.)

well characterized. The technique used by ETI for this mapping is shown in Figure 9. Contour, cross section and depth versus radius plots for TZM are shown in Figures 10, 11 and 12. The same plots for Molybdenum are shown in Figures 13, 14 and 15.

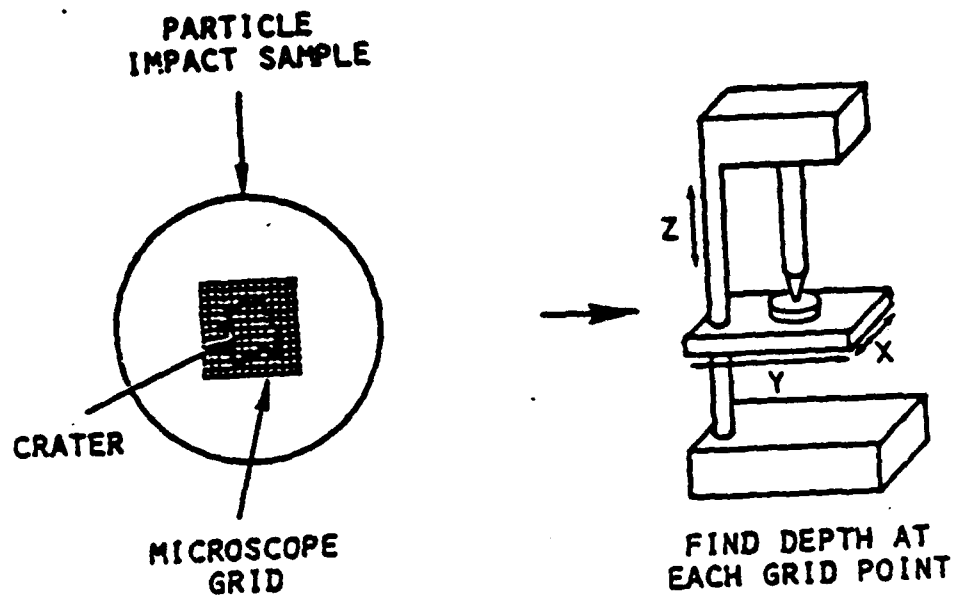
In order to complete the impact test damage assessment, the TZM and Molybdenum specimens from tests E4417 and E4429 were cross-sectioned through the center of the crater. The specimens were then polished and etched and examined at 250X magnification to determine if the base material had experienced any microcracks in the area of the crater. In addition, a series of microhardness measurements were performed to identify if any material changes occurred as a result of impact.

Photomicrographs of the bottom of the crater are shown in Figure 16 for the TZM specimen from Test No. E4417 and Figure 17 for the Molybdenum from Test No. E4429. The diamond shapes, which appear as voids, are indentations from the microhardness measurements. A composite photomicrograph of the crater in the Molybdenum specimen is shown in Figure 18.

The microscopic inspection revealed a difference between the TZM and Molybdenum in grain structure which was not anticipated. The TZM grain structure indicated that recrystallization had occurred but the Molybdenum had not recrystallized. In order to evaluate this condition it was necessary to inspect the grain structure of the TZM and Molybdenum which were tested at 70°F. A photomicrograph of the TZM specimen from Test No. E4422 is shown in Figure 19 and the Molybdenum from test No. E4420 is shown in Figure 20. The grain structure for both materials appear to be normal for mill run stress relieved conditions.

During the microscopic inspection, microcracks were observed in both specimens. The TZM cracks were located about .004 in. below the base of the crater in the center of the specimen (See Figure 19). The microcracks in

Figure 9. Crater Mapping Technique



DATA STORED AND
ANALYZED BY COMPUTER

FIGURE 10

COMPUTER CONTOUR PLOT OF A CRATER
IN TZM RESULTING FROM A 1 MM GLASS
SPHERE IMPACT AT 12.9 kft/sec AND
MATERIAL TEMPERATURE OF 3000° F

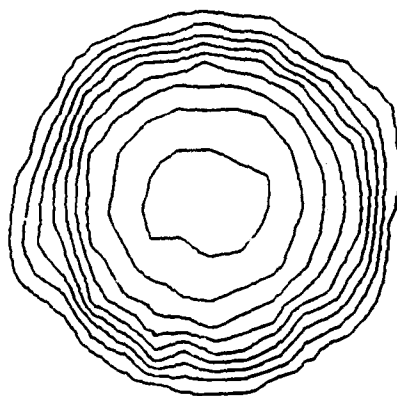
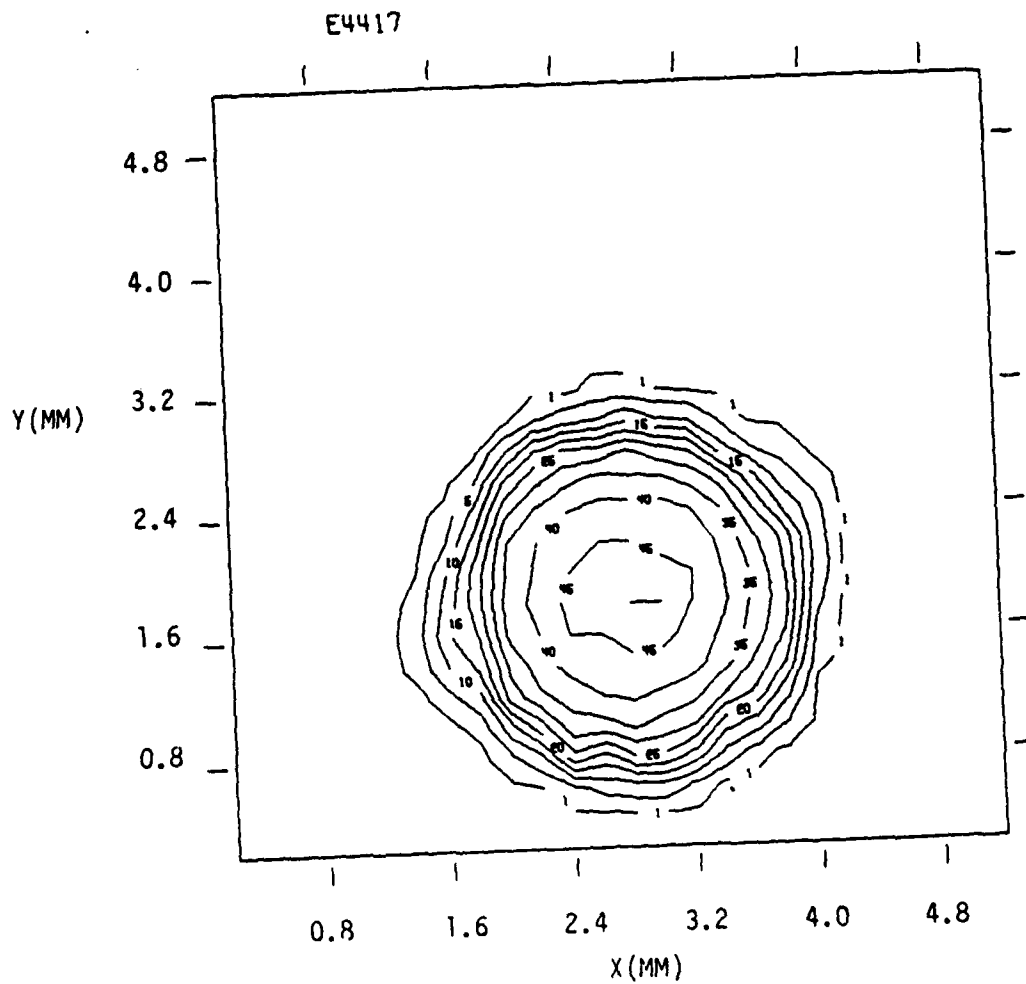


FIGURE 11

COMPUTER PLOT OF CRATER CROSS-SECTIONS
IN THE X-Z AND Y-Z PLANES FOR TZM
RESULTING FROM A 1 MM GLASS SPHERE
IMPACT AT 12.9 kft/sec AND MATERIAL
TEMPERATURE OF 3000°F

E4417

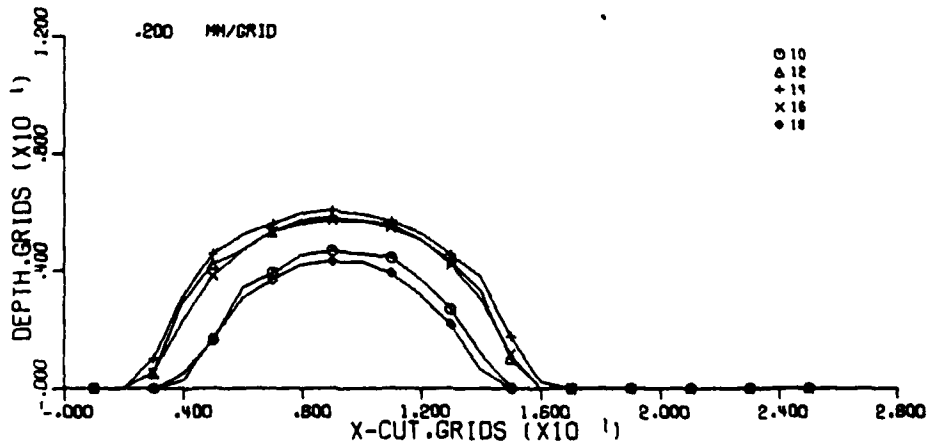
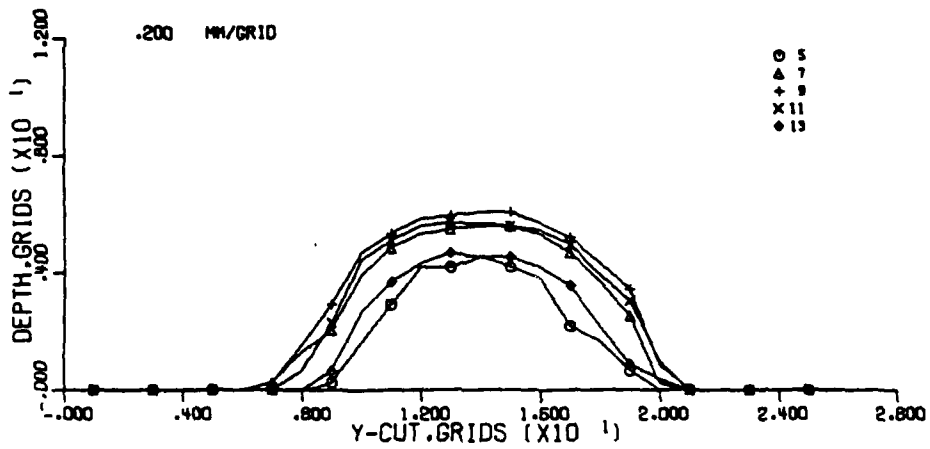


FIGURE 12
DEPTH VERSUS RADIUS PLOT OF CRATER IN TZM

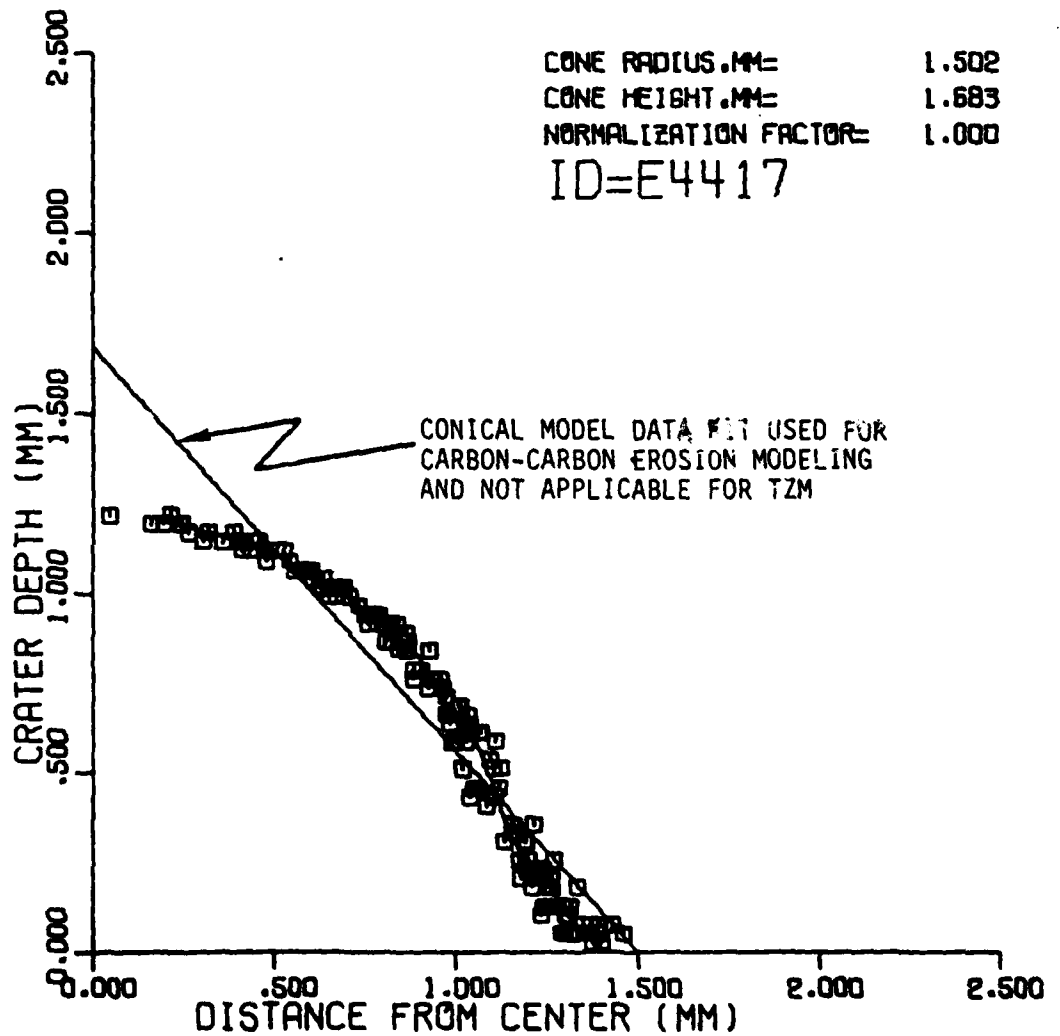


FIGURE 13

COMPUTER CONTOUR PLOT OF CRATER IN MOLYBDENUM
RESULTING FROM A 1 MM GLASS SPHERE IMPACT AT
12.7 kft/sec AND A MATERIAL TEMPERATURE OF 3000°F

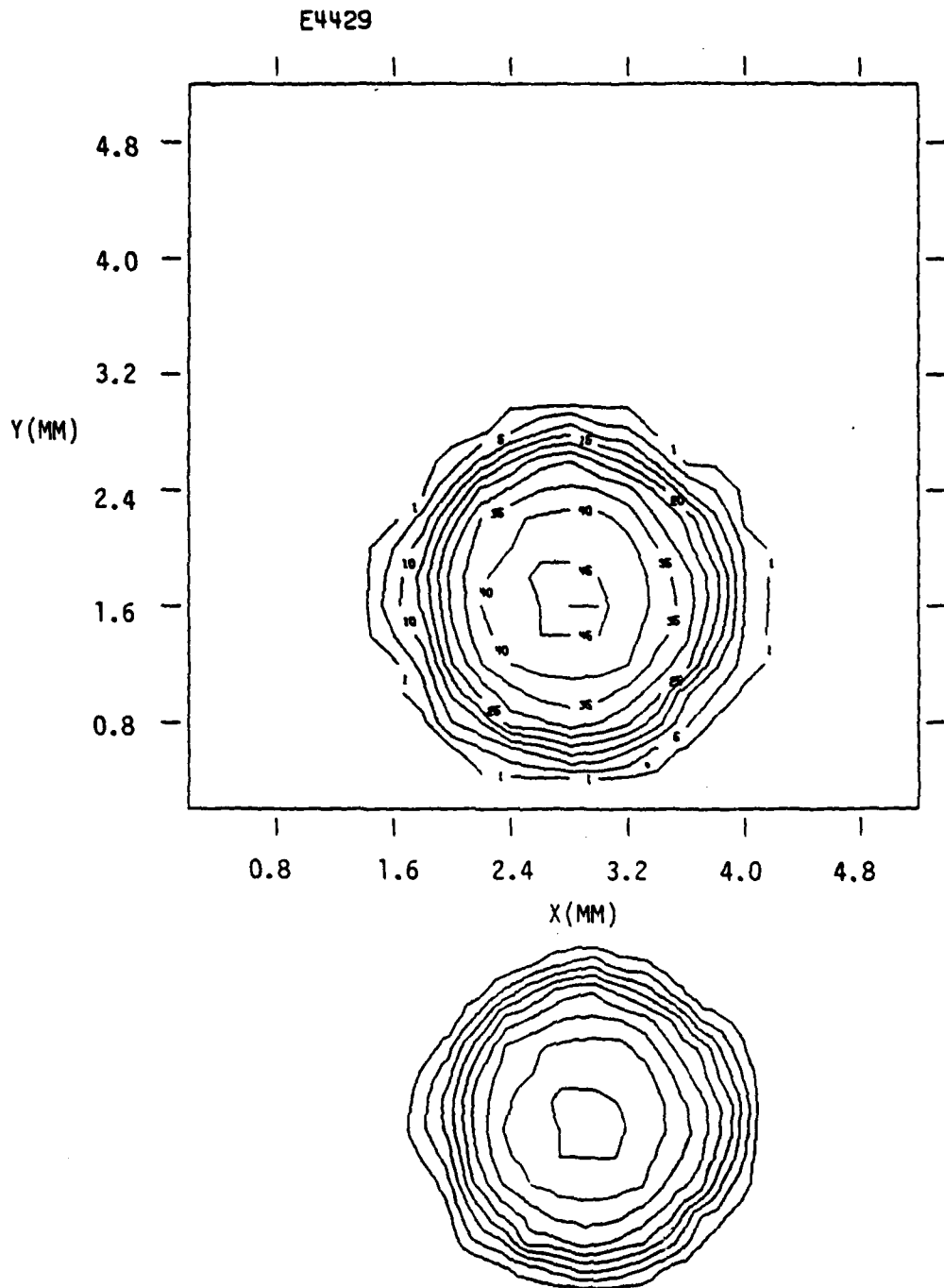


FIGURE 14

COMPUTER PLOT OF CRATER CROSS-SECTIONS IN THE X-Z AND Y-Z PLANES FOR MOLYBDENUM RESULTING FROM A 1 MM GLASS SPHERE AT 12.7 kft/sec AND MATERIAL TEMPERATURE OF 3000°F

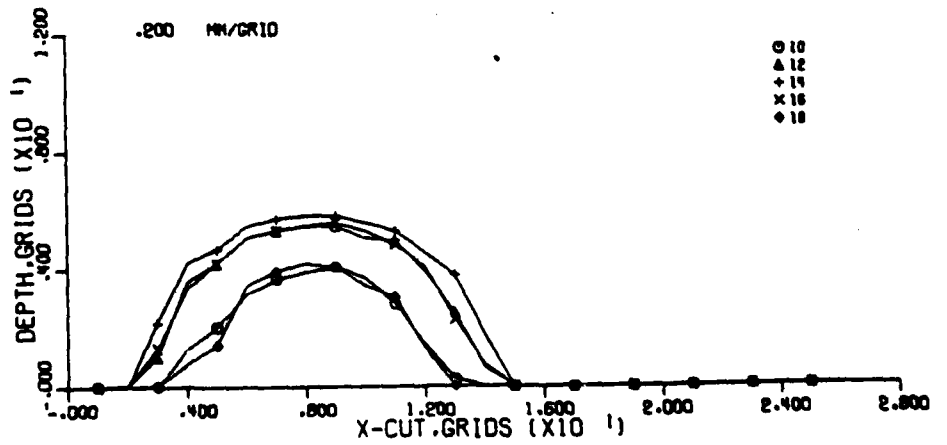
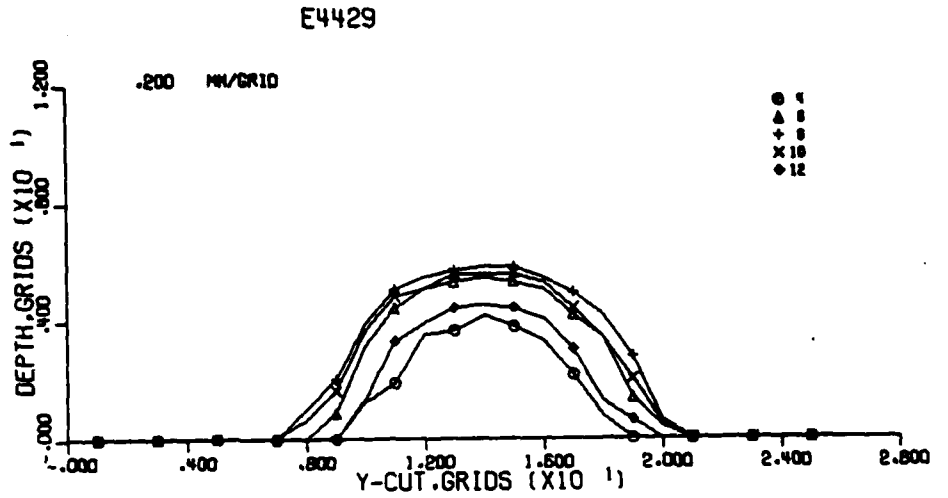
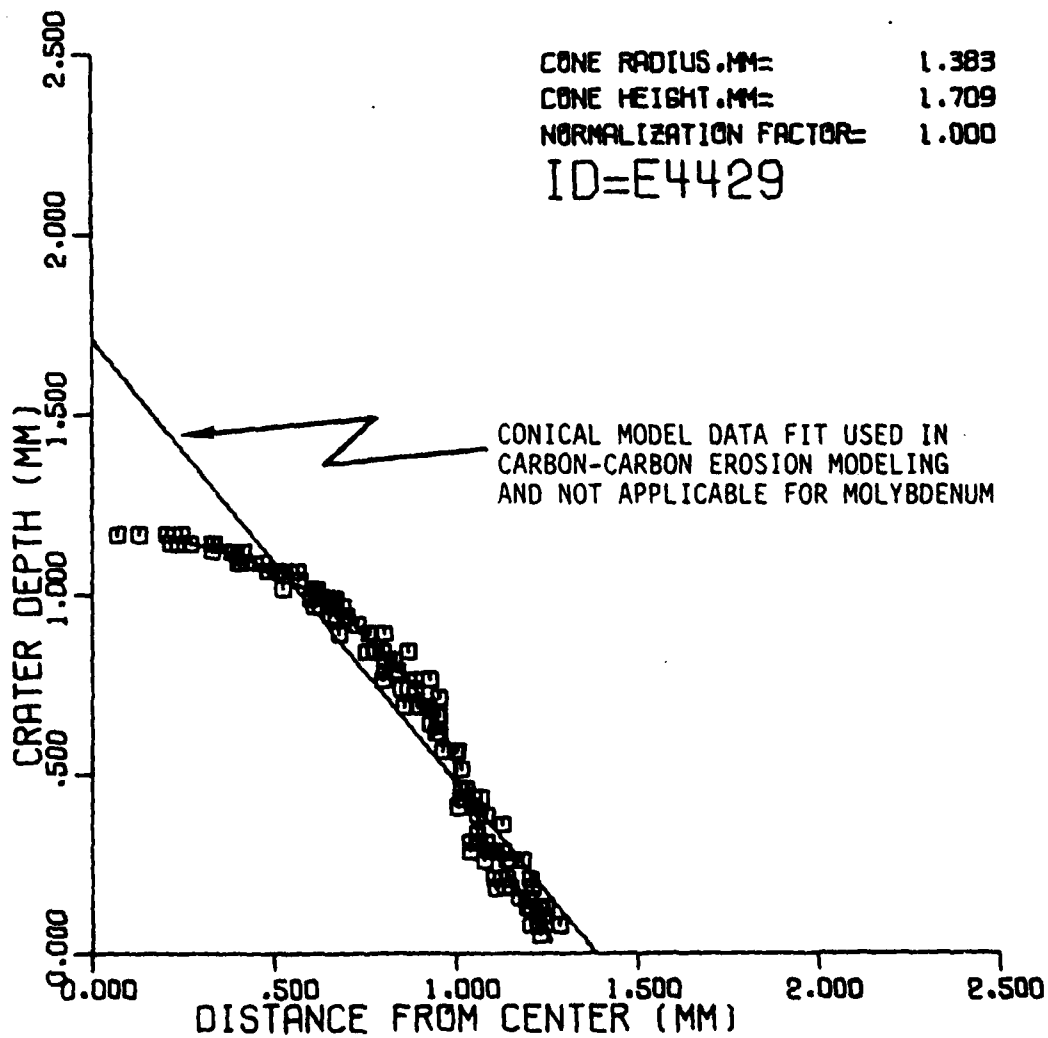


FIGURE 15

DEPTH VERSUS RADIUS PLOT OF CRATER IN MOLYBDENUM



100X ABT-3 #8



Figure 16. Bottom of Crater in TZM 100X

100X ABL-2 #9



Figure 17. Bottom of Crater in Molybdenum 100X

ABL-2 #9 80X



Figure 18. Composite Photomicrograph of Crater in Molybendum 80X Magnification

250X

ABT-3 #9



Figure 19. TZM Specimen from Test E4422 250X

250X

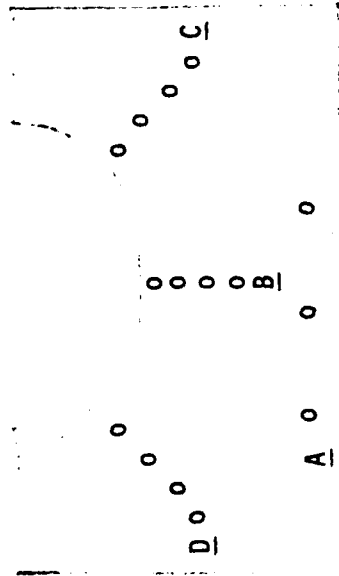
ABL-2 #3



Figure 20. Molybdenum Specimen from Test E4420 250X

TABLE VI

MICROHARDNESS MEASUREMENTS OF TZM AND
MOLYBDENUM TESTS E4417 AND E4429



SPECIMEN BASE

| | A | B | C | D |
|---------------------|-------------------------|----------------------------------|----------------------------------|----------------------------------|
| TZM SPECIMEN | 24 Rc 98 Rb 97 Rb | 95 Rb 94 88 97 | 91 Rb 88 96 93 | 78 Rb 92 88 93 |
| MOLYBDENUM SPECIMEN | 94 Rb 97 95 | 97 Rb 27 Rc 30 Rc 98 Rb | 94 Rb 20 Rc 21 Rc 97 Rb | 91 Rb 24 Rc 24 Rc 94 Rb |

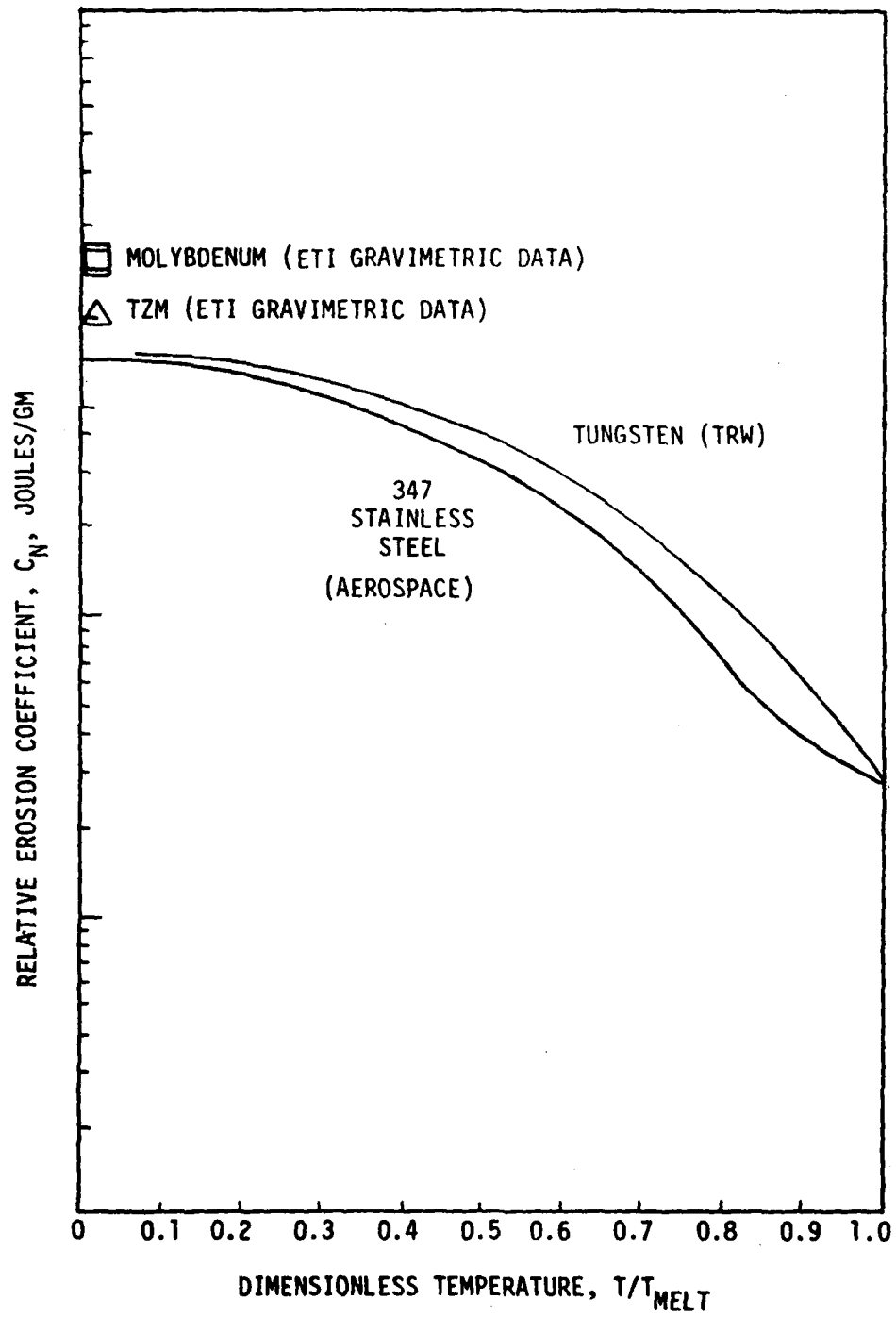


Figure 21. Relative Erosion Coefficients for Molybdenum, TZM, Tungsten and 347 Stainless Steel

the Molybdenum were located approximately halfway up the crater wall and .001 to .004 in. deep (Figure 20). These microcracks do not affect any of the ETI test results.

As a result of the grain structure of the specimens which were tested at ambient temperature, it must be assumed that the recrystallization of the TZM occurred because it was at the elevated test temperature longer than the Molybdenum. Recrystallization of the Molybdenum had started as indicated by the difference in the grain structure from the ambient specimen. The recrystallization or lack of it produces no significant effect on test results since the impact surface temperatures of both materials were the same.

The results of the microhardness measurements are shown in Table VI. These data indicate that the particle impact did not produce any changes in the material in the crater area. All of the hardness readings are within the limits expected in mill run material.

III. CONCLUSIONS AND RECOMMENDATIONS

The results of this test series have indicated that at room temperature (70°F) both TZM and Molybdenum glass bead single particle impact erosion coefficients (C_n) are greater than that established for 347 Stainless Steel. In fact, the room temperature C_n values determined herein are more comparable to and slightly exceed the equivalent value determined from a limited number of similar tests conducted on Tungsten (Figure 21). The elevated temperature C_n values cannot be readily determined from the test data because of the variable oxidation mass loss component which changes as a function of the quantity of residual oxygen present and the dew-point temperature of the inert gas (Argon) purge.

The room temperature erosion coefficients derived from this investigation can be used as a crude indicator of the flight weather induced erosion performance characteristics of these high temperature refractory materials. If similar C_n vs. temperature relationships are assumed for these metals in

comparison to 347 stainless steel, relative or normalized erosion performance can be predicted. However, as evidenced from AEDC Track G test data for Stainless Steel in both dust and snow particle environments, single particle glass data does not accurately reflect hyperballistic range erosion characteristics.

In order to obtain more relevant erosion performance data for these materials, TCNT weather testing in Track G at high pressures is recommended. This ground test method is more representative of flight conditions, and would include the benefits of testing with multiple particle impacts, snow rather than glass, testing a porous surface rather than a solid surface, and the effect of blowing with an active coolant. While multiple particle impact data can be obtained from a hypervelocity projectile launched erosion test facility, extrapolation of this data to flight performance conditions is difficult at best, and therefore cannot be recommended.

DISTRIBUTION LIST

DARPA/STO (Col Wes Kurowski) (1 copy)
1400 Wilson Boulevard
Arlington, VA 22209

General Electric Company (2 copies)
ATTN: Bob Neff
3198 Chestnut Street
Philadelphia, PA 19101

AVCO Corporation (1 copy)
ATTN: Mr. Noel Thyson
201 Lowell Street
Wilmington, MA 01887

TRW (1 copy)
ATTN: Mr. Mike Gyetvay
Bldg. 88, Room 1012
One Space Park
Redondo Beach, CA 90278

PDA Engineering (1 copy)
ATTN: Mr. John Stetson
1560 Brookhollow Drive
Santa Ana, CA 92705

**DA
FILM**